Novel α-Hydroxy γ-Butenolides of Kelp Endophytes Disrupt Bacterial Cell-to-Cell Signaling

Marine Vallet, Yee-Meng Chong, Anne Tourneroche, Grégory Genta-Jouve, Cédric Hubas, Raphaël Lami, Claire M M Gachon, Tatyana A Klochkova, Kok-Gan Chan, Soizic Prado

frontiers in Marine Science

ORIGINAL RESEARCH
published: 30 July 2020
doi: 10.3389/fmars.2020.00601

Novel α-Hydroxy γ-Butenolides of Kelp Endophytes Disrupt Bacterial Cell-to-Cell Signaling

*Marine Vallet[1,2†], Yee-Meng Chong[3†], Anne Tourneroche[1], Grégory Genta-Jouve[1,4], Cédric Hubas[5], Raphael Lami[6], Claire M. M. Gachon[1,7], Tatyana Klochkova[8], Kok-Gan Chan[3,9] and Soizic Prado[1]**

[1] Muséum National d'Histoire Naturelle, Unité Molécules de Communication et Adaptation des Micro-Organismes (UMR 7245), CNRS, Sorbonne Université, Paris, France, [2] Research Group Plankton Community Interaction, Max Planck Institute for Chemical Ecology, Jena, Germany, [3] Division of Genetics and Molecular Biology, Faculty of Science, Institute of Biological Sciences, University of Malaya, Kuala Lumpur, Malaysia, [4] Laboratoire de Chimie-Toxicologie Analytique et Cellulaire (C-TAC), UMR CNRS 8638 COMETE, Université Paris Descartes, Paris, France, [5] UMR Biologie des Organismes et des Ecosystèmes Aquatiques, CNRS 7208-MNHN-UPMC-IRD 207-UCN-UA, Paris, France, [6] CNRS, Laboratoire de Biodiversité et Biotechnologies Microbiennes (LBBM), Observatoire Océanologique, Sorbonne Université, Banyuls-sur-Mer, France, [7] The Scottish Association for Marine Science, Scottish Marine Institute, Oban, United Kingdom, [8] Department of Science and Innovations, Kamchatka State Technical University, Petropavlovsk-Kamchatsky, Russia, [9] International Genome Centre, Jiangsu University, Zhenjiang, China

OPEN ACCESS

Edited by:
Angel Borja, Technological Center Expert in Marine and Food Innovation (AZTI), Spain

Reviewed by:
Perumal Karthick, Sea6 Energy Pvt Ltd., India
Hanzhi Lin, University of Maryland Center for Environmental Science (UMCES), United States

***Correspondence:**
Soizic Prado
sprado@mnhn.fr;
soizic.prado@mnhn.fr

† These authors have contributed equally to this work

Specialty section:
This article was submitted to Marine Ecosystem Ecology, a section of the journal Frontiers in Marine Science

Received: *05 December 2019*
Accepted: *30 June 2020*
Published: *30 July 2020*

Citation:
Vallet M, Chong Y-M, Tourneroche A, Genta-Jouve G, Hubas C, Lami R, Gachon CMM, Klochkova T, Chan K-G and Prado S (2020) Novel α-Hydroxy γ -Butenolides of Kelp Endophytes Disrupt Bacterial Cell-to-Cell Signaling. Front. Mar. Sci. 7:601. doi: 10.3389/fmars.2020.00601

A wide range of microbial symbionts such as bacteria and fungi colonize the tissues of macrophytes. The chemical interactions between these endophytes remain underexplored. The obligate marine fungus *Paradendryphiella salina* was isolated from several healthy brown macrophyte species. Novel α-hydroxy γ-butenolides produced by *P. salina* were purified and characterized by nuclear magnetic resonance (NMR). These compounds interfere with the bacterial quorum sensing system as shown in bioassays with pathogenic bacterial model *Pseudomonas aeruginosa*. Ultra-performance liquid chromatography–high-resolution mass spectrometry (UHPLC-HRMS)-based comparative metabolomics revealed the presence of the main α-hydroxy γ-butenolides among all the *P. salina* strains isolated from different hosts as well as a high metabolic variability related to the alga-host species. Collectively, these findings highlight the key role of microbial chemical signaling that may occur within the algal holobiont.

Keywords: fungal endophytes, marine macrophytes, endomicrobiota, *Paradendryphiella salina*, α-hydroxy γ-butenolide, quorum sensing, quorum quenching

INTRODUCTION

Marine macrophytes harbor a wide range of mutualistic microorganisms that contribute to their host health through their life cycle and are involved in maintaining the physiological status of their host (Wahl et al., 2012; Egan et al., 2013; Singh and Reddy, 2015). For instance, seaweed-associated bacteria have profound effects on their development, nutrition, and defense (Wichard et al., 2015; Tapia et al., 2016). Filamentous fungi can also colonize asymptomatically the tissues of seemingly healthy seaweeds, but their ecological function often remains unclear (Debbab et al., 2012). Nevertheless, these fungi can produce bioactive metabolites that can kill algal pathogens such as protistan parasites, suggesting that their functions in their host might be carried on by chemical signaling (Vallet et al., 2018). Among the chemicals involved in the communication driving the microbial interactions, quorum sensing (QS), a mechanism allowing bacteria to coordinate gene expression according to specific signaling molecules, is of particular interest. Indeed, QS may regulate the expression

of genes involved in colonization processes or virulence including biofilm formation as well as toxin production (Atkinson and Williams, 2009). QS thus requires the synthesis, exchange, and perception of bacterial signaling molecules, named autoinducers (AI). Recently, this mechanism has also been described in eukaryotes, particularly in fungi, where they regulate processes such as pathogenesis, sporulation, morphological differentiation, secondary metabolite production, and biofilm formation (Barriuso et al., 2018). Of note is that fungi in the environment are often competing with bacteria thus hinting at an inter-kingdom chemical signaling system and may produce inhibitors of bacterial QS (Deveau et al., 2018). This process is referred to as quorum quenching and can change the synthesis, release, accumulation, or recognition of the QS signals (Dong et al., 2001). Therefore, we previously reported chemicals isolated from the kelp endomicrobiota which had an impact on bacterial QS (Tourneroche et al., 2019) and demonstrated that metabolites produced by certain fungi endophytic to brown algae were able to inhibit bacterial QS (Tourneroche et al., 2019).

Here, the obligate marine fungus *Paradendryphiella salina* was isolated from healthy-looking tissues of several brown macrophytes species, such as *Saccharina latissima*, *Laminaria digitata*, *Pelvetia canaliculata,* and *Ascophyllum nodosum* in French and Scottish coasts. The fungal extracts exhibited potent quorum quenching abilities (Tourneroche et al., 2019). We thus elucidated the chemical identity of the metabolites responsible for the observed bioactivity using one strain isolated from *L. digitata*. Four novel α-hydroxyl γ-butenolides (**1**-**4**) were purified and characterized by nuclear magnetic resonance (NMR). The metabolites dramatically reduced the virulence of the pathogenic bacteria *Pseudomonas aeruginosa* by targeting specifically the quorum-sensing systems. Furthermore, mass spectrometry (MS)-based metabolomics highlighted the presence of α-hydroxyl γ-butenolides among the *P. salina* strains as well as a host-specificity of *P. salina* metabolomes.

RESULTS

Chemical Investigation of *Paradendryphiella salina* LD40H

To identify the features found in the metabolomics analysis, *P. salina* strain LD40H was cultivated at large scale, and its metabolites were purified and identified with standard natural product approaches. Compound **1** (**Figure 1**) was isolated as a yellow solid with an $[\alpha]^{24}_{D}$ of +12 (*c* 0.5, MeOH). The molecular formula $C_{12}H_{10}O_5$ was deduced from the molecular peak at *m/z* 235.0610 $[M + H]^+$ in HR-ESI-MS (cald 235.0606 for $C_{12}H_{11}O_5$). The IR spectrum pointed out three absorptions at 1747 cm^{-1}, 1620 cm^{-1}, and 3336 cm^{-1}, suggesting the presence of one α, β unsaturated lactone carbonyl function group, one carbonyl group, and one hydroxyl group, respectively. The ^1H NMR spectrum of **1** exhibited five aromatic protons (δ_H 7.70–7.30 ppm) and one methyl singlet (δ_H 1.75 ppm) (**Supplementary Table S1**). The ^{13}C NMR spectrum displayed 10 sp^2 signals including two carbonyls at δ_C 170.3 and 172.4 and two sp^3 carbons for which one oxygenated carbon at δ_C 85.2 ppm and one methyl at δ_C 22.0 ppm (**Supplementary Table S1**). The heteronuclear multiple bond correlation (HMBC) spectrum pointed out correlations between the methyl singlet H-6 at δ 1.75 and the carbonyl C-5 at δ_C 172.4, the oxygenated tetrasubstituted carbon C-4 at δ_C 85.2, and the carbon C-3 at δ_C 131.2 ppm. In addition, HMBC correlations between aromatics protons H2′/H6′ and the carbon C-3 enabled to attach the aromatic cycle on the previously described motif. Finally, a long-range correlation between a methyl singlet at H-6 at δ 1.75 with the carbonyl C-2 at δ_C 140.7 allowed to define a lactone ring and to propose an enol function in C-2. Furthermore, this hydroxyl was detected on the ^1H spectrum performed in $CDCl_3$. Consequently, the structure of **1** was determined to be an α-hydroxyl γ butenolide (**Figure 1**) and was named dendryphiellone A. The structure of compound **2** was found to be closely related to structure **1**. Indeed, the molecular formula of **2** was determined as $C_{13}H_{12}O_5$ by positive mode HR-ESI-MS (*m/z* 249.0748 $[M + H]^+$). The ^1H and ^{13}C NMR spectra of **2** were very similar to those of **1**, differing solely by the presence of an additional methoxy C-7 at δ_C 53.8 ppm and δ_H 3.79 (**Supplementary Table S1**). HMBC correlations between the methoxy and the carbonyl at δ_C 172.4 suggested thus the presence of a methyl ester in C-5 instead of the carboxylic acid in the compound **1**. We thus gave the name dendryphiellone B to compound **2** (**Figure 1**). Compound (**3**) was isolated as a yellow amorphous solid. Its molecular formula was established as $C_{12}H_{13}O_4$, based on its HR-ESI-MS spectra which shows a molecular ion at *m/z* 221.0809 $[M + H]^+$. The ^1H and ^{13}C NMR data of **3** (**Supplementary Table S1**) revealed that this compound was very similar to compounds **1**-**2** except the presence of a dioxygenated carbon at δ_C 108.9 and a methoxy singlet at δ_H 3.16. The HMBC spectrum

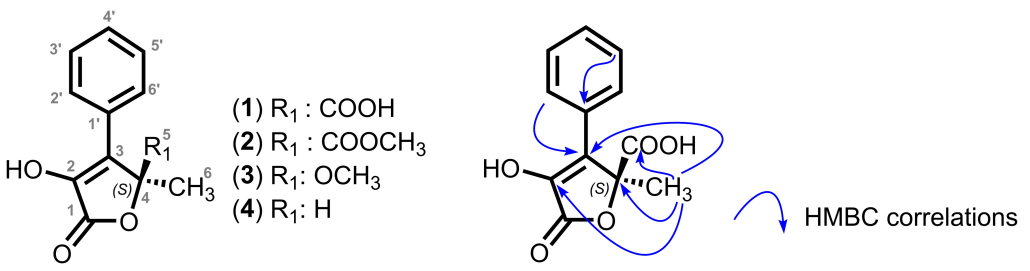

FIGURE 1 | Structures of the dendryphiellones A-D (**1**-**4**) and key HMBC correlations for the dendryphiellone A.

highlighted strong correlations between both the methoxy δ_H 3.16 and the methyl at δ_H 1.72 and the oxygenated carbon at δ_C 108.9, thus leading to the structural determination of **3** as a new compound and named dendryphiellone C (**Figure 1**). Compound (**4**) was isolated as a brown amorphous powder with an $[\alpha]_D$ of +10 (MeOH, *c* 0.5). The molecular formula $C_{11}H_{11}O_3$ was deduced from the molecular peak at *m/z* 191.0698 $[M + H]^+$ in HR-ESI-MS (191.0708, calcd. for $C_{11}H_{11}O_3$). Comparison of the ^1H and ^{13}C NMR data of compound **4** revealed a structure related to dendryphiellones **1-3**. The ^{13}C NMR spectra exhibited the 11 carbons of the formula including the carbonyl C-1 at δ_C 170.1. However, the C-4 carbon present in compounds **1-3** was replaced by an oxymethine at δ_C 76.3. This was confirmed on the ^1H NMR data exhibiting the presence of an oxymethine at δ_H 5.47 ppm represented as a quadruplet. The $H^{-1}H$ correlation spectroscopy (COSY) spectrum exhibited also a spin system including the methyl C-5 and the oxymethine H-4 suggesting the absence of carbonyl function in position γ of the butenolide as for compounds **1-3**. This was confirmed by HMBC correlations between H-4 at δ_H 5.47 ppm and C-1, C-2, and C-3 at 170.1, 136.4, and 131.2 ppm, respectively. Altogether, these results allowed proposing the structure for compound **4**. Racemic of this compound **4** has been previously synthesized but the stereochemistry was not characterized so far (Zask, 1992). The absolute configuration was thus determined by comparing the calculated value of the optical rotation, taking advantage of the relatively simple structure of **1-4** as described in Komlaga et al. (2017). In order to measure the accuracy of the prediction on this family of compounds, the optical rotation of two similar compounds was predicted and the results are listed in **Supplementary Table S2**. The density functional theory (DFT) values of the optical rotation were in agreement with the experimental ones both in terms of sign and amplitude for the two examples. The calculation was then performed for compounds **1**-**4** and presented in **Supplementary Table S2**.

Although greater than the experimental values, the DFT predicted optical rotations signs were in agreement with an *S* configuration for all compounds. This absolute configuration was further confirmed by the sign of the optical rotation of a very similar compound, (*S*)-(+)-5-methyl-4-phenylfuran-2-(5H)-one of which the asymmetric synthesis was realized (Krawczyk et al., 2007).

Assessment of Quorum Quenching Abilities of Dendryphiellones (1-4)

A preliminary screen for QS inhibition was conducted with the dendryphiellones A-D (**1-4**) using *Chromobacterium violaceum* CV026. Wild-type *C. violaceum* produces violet colonies on solid media due to its inherent ability to synthesize the antibiotic violacein which is controlled by the QS and regulated by the major C6-HSL. A significant decrease in violacein production, comparable to the activity of the positive control furanone, was observed in the presence of four compounds of dendryphiellones (**Figure 2A**). To ensure that the decrease of the QS activity was not due to bactericidal activity against the QS biosensor *C. violaceum* CV026, the dendryphiellones were also tested on the growth of *C. violaceum* CV026 (**Supplementary Figure S5**). No bactericidal or bacteriostatic effects were observed suggesting that dendryphiellones significantly reduce the QS-regulated virulence in the bacteria/biosensors without affecting the viability of the biosensor used in this experiment.

The dendryphiellones A-D (**1-4**) were further subjected to a bioluminescence assay with two *lux*-based biosensors, *Escherichia coli* [pSB401] and *E. coli* [pSB1075]. Synthetic 3-oxo-C6-HSL was added into *E. coli* [pSB401], while *E. coli* [pSB1075] requires synthetic 3-oxo-C10-HSL to induce the bioluminescence (Winson et al., 1995). The addition of dendryphiellones A-D (**1-4**) significantly impacted the bioluminescence activity of both biosensors (**Figures 2C,D**). These results support the hypothesis that the dendryphiellones could interfere in QS systems involving both short- and long-chain N-acylhomoserine lactone (AHL). Furthermore, since these biosensors exhibit a defective *luxI* synthase gene, the QS mechanisms of the dendryphiellones suggest to not involve the inhibition of AHLs synthesis.

On the other hand, the dendryphiellones were assessed on *P. aeruginosa* strain PAO1, a bacterial model for QS studies. This strain is a known human opportunistic pathogen that has the ability using QS process in order to regulate various virulence factors such as motility, bioluminescence, biofilm maturation, and production of antibiotics. It produces various QS-related virulence determinants, including the release of secondary metabolites such as exotoxin A and pyocyanin (Miller and Bassler, 2001; Henke and Bassler, 2004; Williams, 2007). The addition of compounds **1-4** considerably reduced the pyocyanine bacterial virulence factor (**Figure 2B**). Since the swarming in *P. aeruginosa* PAO1 is also regulated by the QS system, the dendryphiellones A-D (**1-4)** were also tested for their ability to inhibit the swarming motility of the bacteria. As depicted in **Figure 2E**, the swarming inhibition of compounds **1-4** is closely similar to the effect of positive control using furanone.

Metabolomic Investigations of *Paradendryphiella salina*

In order to evaluate the distribution of the dendryphiellones A-D (**1-4**) among the *P. salina* strains isolated from *A. nodosum* (AN), *L. digitata* (LD), *P. canaliculata* (PC), and *S. latissima* (SL), the metabolome of the nine strains was analyzed by LC-MS. Raw MS data were treated with XCMS package under R environment and gave a primary dataset with 27170 *m/z* features. To limit noise from compounds already present in culture media, the dataset was filtered with an in-house script to retain only features endowed with an intensity fivefold more than their average intensity in blank samples in at least one sample. This filtering process yielded 12050 variables. The PCA score plot for all samples displayed a homogeneous pattern of quality control (QC) samples and blanks indicating the stability and repeatability of the analytical instrument. Taking into account only algal samples (i.e., AN, LD, SL, and PC), a between-class analysis (BCA) analysis was performed which clearly indicated a clustering of the chemical profiles of the *P. salina* metabolome extracts according to the hosting algae (algal host, as a factor, explained 26.3% of the total inertia of the unsupervised PCA) (**Figure 3**). The two first

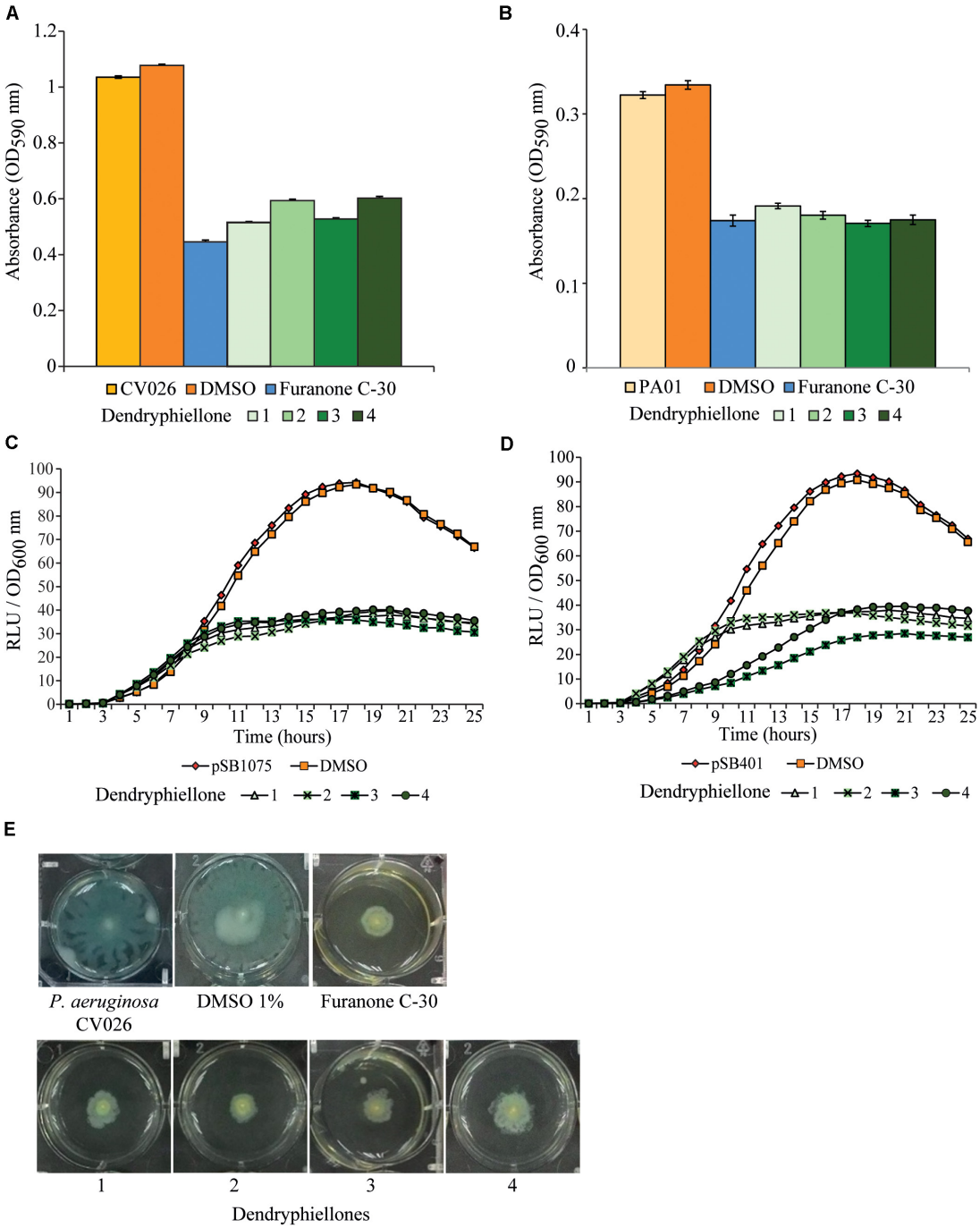

FIGURE 2 | Functional bioassays attesting of the quorum quenching abilities the dendryphiellones **1-4**. **(A)** Inhibition of violacein production in *C. violaceum* CV026 in the presence of the four compounds. **(B)** Effects of the compounds against the production of pyocyanin in *P. aeruginosa* PAO1. **(C)** Inhibition of *lux*-based biosensors by the compounds **1-4** in *E. coli* [pSB401] and **(D)** *E. coli* [pSB1075]. **(E)** Swarming assays against *P. aeruginosa* PAO1 (1) supplemented with 1% (*v/v*) DMSO and 15 μg mL^{-1} of (3) furanone C-30, (4) dendryphiellone A, (5) dendryphiellone B, (6) dendryphiellone C, and (7) dendryphiellone D.

components of the BCA explained 46.9 and 31.6%, respectively, and were used to test the validity of the ordination according to algal hosts (PerMANOVA, $F = 116.51$, $p < 0.001$). The proportion of total inertia explained raised to 64.9% when taking into account the interaction between algal hosts and fungal strains (result not shown). The first component of the BCA separated *P. salina* metabolome of (SL + LD + AN) from PC (46.9% of the total variance), while the second component allowed the discrimination between *P. salina* metabolome of SL and those of LD + AN + PC (31.6% of the total variance). It is noteworthy

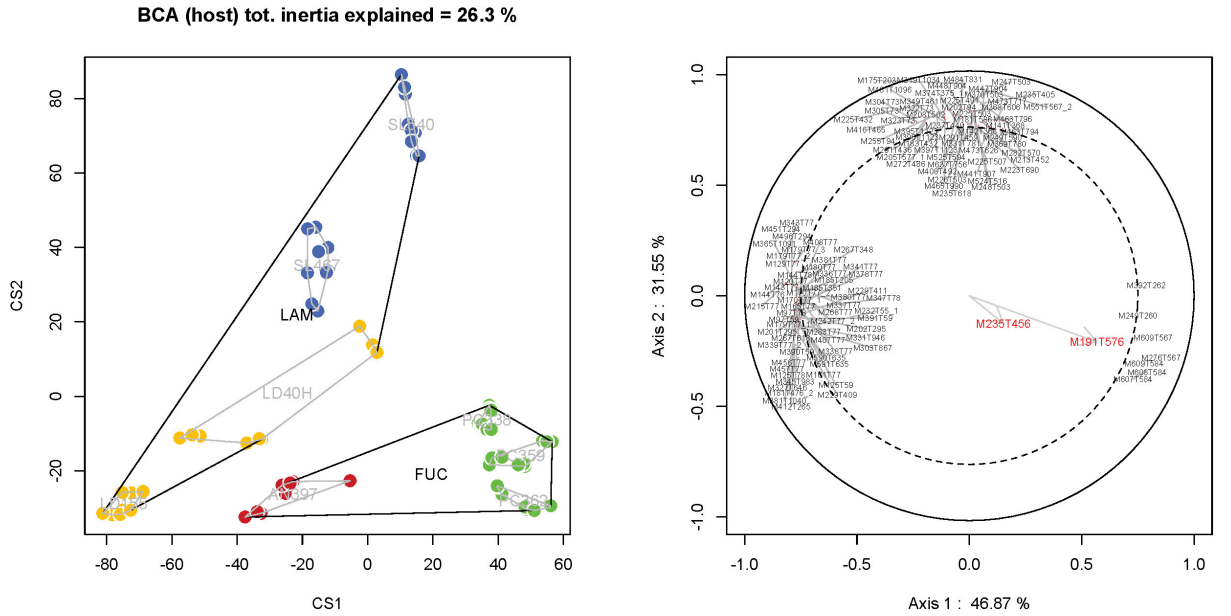

FIGURE 3 | Metabolome structuration of the *P. salina* strains according to the factor host (BCA) and variable importance in projection (VIP) indicating the importance of each *m/z* features in the discrimination between specific sample classes (correlation >0.75) and the distribution of dendryphiellone A (feature M235T456) and dendryphiellone D (M191T576).

that there was a clear separation between fungal metabolomes isolated from Laminariale (SL + LD) and metabolomes obtained from strains isolated from Fucale (AN + PC). Based on the final filtered dataset (12 050 variables), PerMANOVA analyses also showed that *P. salina* metabolome was significantly different between algal hosts (i.e., AN, LD, PC, SL: $F = 12.573$, $p = 0.001$) as well as between Fucales (AN, PC) and Laminariales (LD, SL: $F = 10.035$, $p = 0.001$). Variable importance in projection (VIP) indicating the importance of each *m/z* features in the discrimination between specific sample classes was also evaluated. Metabolites with a correlation lower than 0.75 were not shown in **Figure 3** to improve the readability. Unfortunately, top-ranked metabolites were not unambiguously identified by annotation against ISDB (Allard et al., 2016), GNPS, and MassBank. Similarly, identification against SIRIUS 4.0 (Bocker and Rasche, 2008) and PubChem was inconclusive. Features M235T456 and M191T576 corresponding to dendryphiellone A (**1**) and dendryphiellone D (**4**), respectively, were detected in all the metabolomes of *P. salina* but don't contribute to the discrimination between samples classes (**Figure 3**).

DISCUSSION

The recovery of the cultivable algal holobiont associated with kelps led to the isolation of many strains of *P. salina,* a strictly marine fungus identified with internal transcribed spacer (ITS) sequencing from all four brown algal species investigated (Vallet et al., 2018). This fungal species was first described in the brown macrophyte *Cercospora salina* and was suggested as a saprophytic opportunist (Sutherland, 1916). It was more recently confirmed that *P. salina* is able to degrade alginate, laminarin, and cellulose from brown algae (dela Cruz et al., 2006).

Considering the potential impact of endophytes metabolites on the holobiont function, we undertook the chemical investigation of the secondary metabolites produced by *P. salina*. Accordingly, *P. salina* strain LD40H recovered from the host *L. digitata* was cultivated on a large scale and was extracted to identify the purified compounds and characterize them by MS and NMR. Four new α-hydroxy γ-butenolides named dendryphiellones A-D were thus characterized (**Figure 1**). These compounds feature a 2-furanone core structure which is also present in antifouling butenolides isolated from a marine *Streptomyces* sp. (Zhang et al., 2012; Ding et al., 2018). In addition, a 2-furanone ring is also present in the antifouling halogenated furanones produced by the red macrophyte *Delisea pulchra*, which are involved in the defense against pathogens (Dworjanyn et al., 2006). Indeed, these halogenated furanones are quorum-sensing blockers that are able to inhibit the settlement of invertebrate larvae and algal spores. Furthermore, the bioactivity of the purified dendryphiellones A-D (**1-4**) was assessed against QS activity in a series of functional bioassays. A strong effect of the four dendryphiellones A-D (**1-4**) on the AI-1-mediated QS was observed, and our data support that the dendryphiellones A-D interfere in both bacterial QS systems involving short- and long-chain AHLs. Moreover, the quorum quenching abilities of the dendryphiellones did not involve inhibition AHLs synthesis, since the biosensors exhibited a defective *luxI* synthase gene.

Comparative metabolomics was undertaken with the nine fungal isolates recovered from different host species. As represented in **Figure 3**, dendryphiellones A (**1**) and D (**4**) are produced by all the *P. salina* strains independently of

their host suggesting there are ubiquitous metabolites and key compounds involved in the quorum quenching of *P. salina*. However, (**1**) and (**4**) are not contributing to the discrimination according to the algae host. These findings demonstrate thus that kelps endophytes can produce small molecules that can interfere with bacterial QS, suggesting that chemical signaling is a strong component of the algal holobiont. More tools including QS biosensors built from kelp bacteria would be thus needed to demonstrate the real impact of butenolide on the phycosphere. Unfortunately, no QS biosensor from symbiotic bacteria of *S. latissima* are available so far and their construction would require a lot of hard work including genome sequencing, quantitative polymerase chain reaction (qPCR) and mutants construction. However, our previous works of the microbial diversity highlighted the presence of *P. aeruginosa* strains on kelp phycosphere strengthening thus the possible interaction of butenolides with algal bacterial strains (Tourneroche et al., in revision).

Dendryphiellones A (**1**) and D (**2**) were not detected by LC-MS, while they were isolated and fully characterized in NMR. The absence of detection of compounds **1** and **2** by liquid chromatography-mass spectrometry (LC-MS) might stem from the difference of cultivations between the analytical and preparative scales.

Interestingly, metabolomes varied strongly according to the host origin (**Figure 3**), suggesting that the harboring algae species might have a substantial influence on fungal metabolism. In terrestrial environments, endophytic communities can influence the host plant metabolism by inducing silent gene clusters leading to the synthesis of novel secondary metabolites. On the other hand, there are few studies showing that the host plant can influence the metabolic processes of its endophytes. For instance, lethal genes of virulent symbiont *Nectria haematococca* strains can be induced *in planta* by the host signals homoserine and asparagine (Yang et al., 2005). The endophyte *Neotyphodium lolii* possess high gene expression levels of the toxin Lolitrem when living in its host, but very low levels when cultivated axenically *in vitro*, suggesting that a plant signal is required to induce the metabolite release (Young et al., 2006). Similarly, the complex of phytopathogenic *Heterobasidium* species, which are pine-infecting and non-pine infecting isolates, showed different metabolite patterns according to their hosts (Hansson et al., 2014). In this regard, we suggested that the algal host might influence the expression of the fungal biosynthetic pathways in the kelp endophyte *P. salina*. The difference seen in the metabolomes isolated from *P. salina* according to the order of the hosts, Fucale versus Laminariale, might further uphold this assumption, suggesting that the two orders are producing specific metabolites with direct influence on the fungal metabolome.

Although the chemical signaling occurring in the algal holobiont is not well known, QS processes might be involved in the algal-bacterial symbiotic relationships and might determine the community structure and the health of algal populations. Understanding chemicals-mediated ecological processes will shed light on the intrinsic processes supporting symbiotic interactions between marine macrophytes and their associated microbiota. This understanding requires also the development of new biological tools to answer these outstanding questions. Studying the metabolic expressions of kelp endophytes in wild populations or in aquaculture will grant a deeper understanding of their function and their impacts on the host fitness and performance. As QS is responsible for the significant increase in virulence gene expression in aquaculture farms (Zhao et al., 2015), the novel dendryphiellones A-D might provide a solution to target specific bacterial pathogens.

EXPERIMENTAL SECTION

Strain Cultivation and Metabolites Extraction

The *P. salina* strains AN397T, LD40H, LD155H, PC359H, PC362H, PC338T, SL467H, and SL540T identified from *A. nodosum* (AN), *L. digitata* (LD), *P. canaliculata,* and *S. latissima* (SL) as *P. salina* were cultivated in 90 mm diameter Petri dishes containing 25 mL of MEA medium. Inoculation was performed by spreading spore suspensions (10^4 spores in 100 μL of sterile artificial seawater). The experiment was performed with five biological replicates. Cultures were incubated at 18°C under natural light conditions for 21 days. Cultures of the *P. salina* strains were then cut into pieces and extracted in an ultrasonic bath for 30 min at room temperature after the addition of 30 mL of ethyl acetate. The crude extracts were filtered and dried under vacuum using a centrifugal evaporator.

LC-MS-Based Metabolomic Analysis

The crude extracts were prepared at 0.5 mg mL^{-1} in methanol and 2 μL was injected randomly. The separation occurred onto the C18 Acclaim™ RSLC PolarAdvantage II column (2.1 × 100 mm, 2.2 μm of pore size; Thermo Fisher Scientific, United States) connected to a Dionex Ultimate 3000 HPLC system and coupled to a Maxis II™ QTOF mass spectrometer (Bruker, United States) with an electrospray ionization source. The mobile phases were water (0.1% formic acid) and acetonitrile (0.1% formic acid, solvent B) following a gradient of B at 5, 50, 90, and 5% for 2, 9, 15, and 21 min, respectively. The flow rate was set at 300 μL min^{-1}. The MS parameters were 3.5 Kv of electrospray voltage, 35 psi of nebulizing gas (N_2) pressure, drying gas (N_2) flow rate of 8 L min^{-1}, and 200°C of drying temperature. Mass spectra were recorded at the range of 100–1300 *m*/*z* in positive ion mode.

Raw LC-MS data were calibrated and converted to netCDF format using Data Analysis software (Bruker) and processed using the R package XCMS (Smith et al., 2006). Based on analytical conditions and raw data characteristics, final peak picking parameters were method = "centWave," ppm = 10, and peak width = *c*(5,20), while final grouping parameters were bw = 5, mzwid = 0.015, and retention time correction method = "obiwarp." Other parameters were set to default values. To limit noise from compounds already present in culture media, the dataset was filtered with an in-house script to retain only those features with intensity in at least one sample more than fivefold its average intensity in blank samples.

Statistical Procedures

All analyses and graphs were performed using the R statistical framework (R Core Team, 2019). Principal component analysis (PCA) was used to visualize LC-MS data according to the algal hosts and the fungal strains (using ade4 package, data not shown). Then, between PCA analysis (BCA), a special case of PCA with respect to instrumental variables in which a factor is given as explanatory variable, was used to reveal differences in term of metabolite composition of *P. salina* between algal hosts. BCA analysis performs a decomposition of the total inertia of the unsupervised (PCA) analysis according to a factor (in this case: the algal host). PerMANOVA was used to test the validity of the BCA ordination according to the same explanatory variable used for the BCA computation with a euclidean distance. PerMANOVA was also used (using a Bray-Curtis dissimilarity index) to test significant differences in term of metabolite composition between algal hosts on the filtered dataset (12050 metabolites). Homogeneity of multivariate dispersion was always checked before computing PerMANOVA tests.

Fungal Fermentation and Isolation of Dendryphiellones

Paradendryphiella salina strain LD40H was isolated from the brown macroalga *L. digitata* based on ITS and 28S rDNA sequencing (Vallet et al., 2018). The fungus was grown on 600 mL malt extract agar medium prepared with artificial seawater in 5 L Erlenmeyer flasks and incubated for 24 days at 18°C under a 12 h light: dark photoperiod. The whole cultures were extracted by mechanical stirring in 1 L ethyl acetate three times for 4 h, yielding 3.9 g of crude extract. The extract was subjected to a Gel Sephadex column chromatography using 100% methanol elution, giving 18 sub-fractions. The sub-fraction 5 was further purified on Agilent XDB-C18 Zorbax (21.2 mm × 150 mm, 5 μm) connected to a preparative HPLC using a gradient of water:acetonitrile (0.05% trifluoroacetic acid) of 9:1, 4:1, 1:1, 1:4, 1:9 for 20, 15, 5, 10, and 5 min, respectively. The flow rate was 10 mL min^{-1}. The pure compounds **1**-**4** were detected with UV λ254 nm and collected at 25 min (**1**, 34.6 mg), 33 min (**2**, 3.8 mg), 35 min (**3**, 13.4 mg), and 39 min (**4**, 11.4 mg).

General Experimental Procedures

Nuclear magnetic resonance spectra were recorded at 20°C on a Brucker Advance III HD 400 or 600 MHz (298 K). The ^{1}H and ^{13}C chemical shifts were referenced to the solvent peak of either CD_3OD at δ 3.31 and 4.81 (H_2O), or $CDCl_3$ at δ 7.27. The mass spectra were recorded on an Applied Biosystem QSTAR Pulstar I apparatus (Perkin Elmer) in electrospray ionization (ESI) mode with time of flight (TOF) analysis under a tension of 2500 eV in positive mode. Fourier transform infrared spectroscopy (FTIR) and ultraviolet (UV) spectra were recorded on a Kontron Uvikon 9 × 3W Double Beam (Bioservier, France) spectrometer and a Shimadzu FTIR spectrophotometer 8400S, respectively. Optical rotations were recorded Perkin Elmer 341 polarimeter. The NMR raw spectra are freely available on the Max Planck repository Edmond under the DOI https://dx.doi.org/10.17617/3.3t.

Bacteria Strains and Culture Conditions

The bacterial strains and plasmids used in this study were listed in **Supplementary Table S3**. All the bacteria were grown in Luria–Bertani (LB) medium (Scharlab, Barcelona, Spain) at 37°C, shaking at 220 rpm except for *C. violaceum* CV026 which was cultured at 28°C. Biosensors used in this study are described in the **Supplementary Material**.

Bacterial Growth

The bacterial growth was estimated with previously reported method (Hayouni et al., 2008). Briefly, overnight bacteria cultures were first diluted to $OD_{600\ nm}$ (optical density) of 0.1 before adding into the 96-well microtiter plate which consists of 230 μL of diluted bacteria cultures and 20 μL of samples at 15 μg mL^{-1} concentration. The bacteria were then incubated at their optimum temperature and the optical density $OD_{600\ nm}$ was determined every 30 min for 24 h by Tecan Infinite M200 microplate reader (Switzerland).

Screening of Anti-quorum Sensing Activities

Violacein Assay

The CV026 biosensor was constructed by subjecting *C. violaceum* to mini-Tn*5* transposon mutagenesis in order to attain a double Tn*5* insertion, violacein-negative, white mutant CV026, making it incapable of producing any AHLs. The synthesis of violacein will be restored once the biosensor is supplemented with synthetic C6-HSL exogenously (McClean et al., 1997).

The quantitative analysis of violacein production was performed based on the previously reported method (Chong et al., 2011) with slight modification. Briefly, overnight culture of *C. violaceum* CV026 was adjusted to OD_{600nm} of 1.2 followed by the addition of 0.125 μg mL^{-1} of synthetic C6-HSL (Sigma-Aldrich, United States); 100 μL of CV026 diluted culture was thus transferred into the 96-wells microtiter plate containing 10 μL of samples solubilized in dimethyl sulfoxide (DMSO) at 15 μg mL^{-1}. The microplate was incubated for 16 h at 28°C with the agitation of 220 rpm. The plate was then dried at 60°C until all the medium had evaporated before adding 100 μL of DMSO to each well in order to dissolve the dried violacein. The plate was subsequently incubated for another additional 2 h at 28°C with shaking. The absorbance for each of the well was measured at OD_{590nm} with Tecan Infinite M200 microplate reader (Switzerland). All the experiments were done in triplicate. DMSO (Merck KGaA, Germany) and synthetic furanone C-30 (Sigma-Aldrich, United States) used as negative and positive controls, respectively.

Pyocyanin Assay

Pyocyanin was extracted from the overnight *P. aeruginosa* PAO1 culture supernatant as previously described (Chong et al., 2011). Briefly, 500 μL of samples solubilized at 15 μg mL^{-1} in DMSO were added into 4.5 mL of overnight culture that was diluted to OD_{600nm} of 0.1 and incubated at 37°C for 24 h. The cell culture was thus extracted with 3 mL of chloroform

(Merck KGaA, Germany) and vortexed for 5 min followed by centrifugation at 9000 rpm for 10 min. The chloroform layer was subsequently transferred to a fresh tube and 1 mL of 0.2 M hydrochloric acid (Merck KGaA, Germany) was added by mixing thoroughly. After centrifugation at 9000 rpm for 10 min, the top layer of the mixture was removed and the absorbance was read at 520 nm by using Tecan Infinite M200 microplate reader (Switzerland). All the samples for this assay were done in triplicate. DMSO (Merck KGaA, Germany) and synthetic furanone C-30 (Sigma-Aldrich, United States) served as negative and positive controls, respectively.

Bioluminescence Assay

For bioluminescence assay, the method used was based on the one reported previously (Winzer et al., 2000) with some modification. Both *E. coli* [pSB401] and *E. coli* [pSB1075] cells were grown overnight with shaking in LB medium supplemented with 20 μg mL^{-1} of tetracycline at 37°C. In the 96-well microtiter plate, 20 μL of samples were added into 230 μL of the bacteria culture that was diluted to $OD_{600\,nm}$ of 0.1. Synthetic 3-oxo-C6-HSL (0.001 μg mL^{-1}) and 3-oxo-C10-HSL (0.0125 μg mL^{-1}) (Sigma-Aldrich, United States) were added into *E. coli* [pSB401] and E. *coli* [pSB1075] cultures, respectively. The luminescence and turbidity of the *lux* biosensors were read every 30 min for 24 h with Tecan Infinite M200 microplate reader (Switzerland) at $OD_{600\ nm}$. A graph was plot based on luminescence given in relative light units (RLU) per unit of turbidity ($OD_{600\ nm}$). All the experiments were done in triplicate.

Swarming Motility Assay

The swarming motility assays were done based on the method described previously (Chen et al., 2007) with slight changes. The swarming plate consists of 0.6% (w/v) Bacto^{TM} agar (BD, United States), 0.6% (w/v) Bacto^{TM} Peptone (BD, United States), 0.2% (w/v) yeast extract (BD, United States) and 0.5% (w/v) glucose (Merck, United States) in 1 L of distilled water. Next, 150 μL of samples were mixed together with 5 mL of agar before poured into 6-well plates. The plates were then left to air-dry for 15 min before point inoculated with 1 μL of overnight culture of *P. aeruginosa* PAO1 with OD_{600nm} of 0.1 at the center of the agar surface. The plates were incubated statically at 37°C for 16 h. All the experiments were done in triplicate. DMSO (Merck KGaA, Germany) and synthetic furanone C-30 (Sigma-Aldrich, United States) served as negative and positive controls.

DATA AVAILABILITY STATEMENT

The datasets generated for this study can be found in the **Supplementary Material**.

AUTHOR CONTRIBUTIONS

All authors conceived this study, read, and approved the final manuscript. MV, Y-MC, and AT carried out the experiment and analyzed the data. CH performed the statistical analysis. GG-J made the calculation of optical rotation prediction. MV, SP, and CG wrote the manuscript with the help of CH, K-GC, and RL.

FUNDING

This work was supported by ATM "Microorganisms" grant from the National Museum of Natural History, Paris (SP), PEPS EXOMOD (SP), EC2CO CNRS (SP) and the Mission pour les Initiatives Transverses et Interdisciplinaires (MITI-CNRS) (Défi Adaptation du vivant à son environnement 2020) (SP). The 400 MHz and 600 MHz NMR spectrometers used in this study were funded jointly by the Région Ile-de-France, the MNHN (Paris, France) and the CNRS (France). K-GC thanks the financial support from the University of Malaya (FRGS grant FP022-2018A and HIR grant H-500001-A000027). CG was funded by UKRI GCRF grant number BB/P027806/1. K-GC, Y-MC, and SP thank the French Embassy at Kuala Lumpur, Malaysia, for the fellowships awarded.

SUPPLEMENTARY MATERIAL

The Supplementary Material for this article can be found online at: https://www.frontiersin.org/articles/10.3389/fmars.2020.00601/full#supplementary-material

REFERENCES

Allard, P.-M., Péresse, T., Bisson, J., Gindro, K., Marcourt, L., Pham, V. C., et al. (2016). Integration of molecular networking and in-silico MS/MS fragmentation for natural products dereplication. *Anal. Chem.* 88, 3317–3323. doi: 10.1021/acs.analchem.5b04804

Atkinson, S., and Williams, P. (2009). Quorum sensing and social networking in the microbial world. *J. R. Soc. Interf.* 6, 959–978. doi: 10.1098/rsif.2009.0203

Barriuso, J., Hogan, D. A., Keshavarz, T., and Martinez, M. J. (2018). Role of quorum sensing and chemical communication in fungal biotechnology and pathogenesis. *FEMS Microbiol. Rev.* 42, 627–638. doi: 10.1093/femsre/fuy022

Bocker, S., and Rasche, F. (2008). Towards de novo identification of metabolites by analyzing tandem mass spectra. *Bioinformatics* 24, i49–i55. doi: 10.1093/bioinformatics/btn270

Chen, B. G., Turner, L., and Berg, H. C. (2007). The wetting agent required for swarming in *Salmonella enterica* serovar typhimurium is not a surfactant. *J. Bacteriol.* 189, 8750–8753. doi: 10.1128/JB.01109-07

Chong, Y. M., Yin, W. F., Ho, C. Y., Mustafa, M. R., Hadi, A. H., Awang, K., et al. (2011). Malabaricone C from Myristica cinnamomea exhibits anti-quorum sensing activity. *J. Nat. Prod.* 74, 2261–2264. doi: 10.1021/np100872k

Debbab, A., Aly, A. H., and Proksch, P. (2012). Endophytes and associated marine derived fungi—ecological and chemical perspectives. *Fungal Divers.* 57, 45–83. doi: 10.1007/s13225-012-0191-8

dela Cruz, T. E., Schulz, B. E., Kubicek, C. P., and Druzhinina, I. S. (2006). Carbon source utilization by the marine *Dendryphiella* species *D. arenaria* and *D. salina*. *FEMS Microbiol. Ecol.* 58, 343–353. doi: 10.1111/j.1574-6941.2006.00184.x

Deveau, A., Bonito, G., Uehling, J., Paoletti, M., Becker, M., Bindschedler, S., et al. (2018). Bacterial-fungal interactions: ecology, mechanisms and challenges. *FEMS Microbiol. Rev.* 42, 335–352. doi: 10.1093/femsre/fuy008

Ding, W., Ma, C., Zhang, W., Chiang, H., Tam, C., Xu, Y., et al. (2018). Anti-biofilm effect of a butenolide/polymer coating and metatranscriptomic analyses. *Biofouling* 34, 111–122. doi: 10.1080/08927014.2017.1409891

Dong, Y. H., Wang, L. H., Xu, J. L., Zhang, H. B., Zhang, X. F., and Zhang, L. H. (2001). Quenching quorum-sensing-dependent bacterial infection by an N-acyl homoserine lactonase. *Nature* 411, 813–817. doi: 10.1038/35081101

Dworjanyn, S. A., Wright, J. T., Paul, N. A., De Nys, R., Steinberg, P. D., and Larsson, S. (2006). Cost of chemical defence in the red alga *Delisea pulchra*. *Oikos* 113, 13–22.

Egan, S., Harder, T., Burke, C., Steinberg, P., Kjelleberg, S., and Thomas, T. (2013). The seaweed holobiont: understanding seaweed–bacteria interactions. *FEMS Microbiol. Rev.* 37, 462–476. doi: 10.1111/1574-6976.12011

Hansson, D., Wubshet, S., Olson, Å, Karlsson, M., Staerk, D., and Broberg, A. (2014). Secondary metabolite comparison of the species within the Heterobasidion annosum s.l. complex. *Phytochemistry* 108, 243–251. doi: 10.1016/j.phytochem.2014.08.028

Hayouni, E. A., Bouix, M., Abedrabba, M., Leveau, J.-Y., and Hamdi, M. (2008). Mechanism of action of *Melalueca armillaris* (sol. ex gaertu) sm. essential oil on six lab strains as assessed by multiparametric flow cytometry and automated microtiter-based assay. *Food Chem.* 111, 707–718. doi: 10.1016/j.foodchem.2008.04.044

Henke, J. M., and Bassler, B. L. (2004). Three parallel quorum-sensing systems regulate gene expression in Vibrio harveyi. *J. Bacteriol.* 186, 6902–6914. doi: 10.1128/jb.186.20.6902-6914.2004

Komlaga, G., Genta-Jouve, G., Cojean, S., Dickson, R. A., Mensah, M. L. K., Loiseau, P. M., et al. (2017). Antiplasmodial Securinega alkaloids from *Phyllanthus fraternus*: discovery of natural (+)-allonorsecurinine. *Tetrahedron Lett.* 58, 3754–3756. doi: 10.1016/j.tetlet.2017.08.045

Krawczyk, E., Koprowski, M., and Luczak, J. (2007). A stereoselective approach to optically active butenolides by Horner–Wadsworth–Emmons olefination reaction of α-hydroxy ketones. *Tetrahedron Asymmetry* 18, 1780–1787. doi: 10.1016/j.tetasy.2007.07.027

McClean, K. H., Winson, M. K., Fish, L., Taylor, A., Chhabra, S. R., Camara, M., et al. (1997). Quorum sensing and Chromobacterium violaceum: exploitation of violacein production and inhibition for the detection of N-acylhomoserine lactones. *Microbiology* 143, 3703–3711. doi: 10.1099/00221287-143-12-3703

Miller, M. B., and Bassler, B. L. (2001). Quorum sensing in bacteria. *Annu. Rev. Microbiol.* 55, 165–199.

R Core Team (2019). *R: A Language and Environment for Statistical Computing*. Vienna: R Foundation for Statistical Computing.

Singh, R. P., and Reddy, C. R. (2015). Unraveling the functions of the macroalgal microbiome. *Front. Microbiol.* 6:1488. doi: 10.3389/fmicb.2015.01488

Smith, C. A., Want, E. J., O'Maille, G., Abagyan, R., and Siuzdak, G. (2006). XCMS: processing mass spectrometry data for metabolite profiling using nonlinear peak alignment, matching, and identification. *Anal. Chem.* 78, 779–787. doi: 10.1021/ac051437y

Sutherland, G. K. (1916). Marine fungi imperfecti. *New Phytol.* 15, 35–48. doi: 10.1111/j.1469-8137.1916.tb07201.x

Tapia, J. E., Gonzalez, B., Goulitquer, S., Potin, P., and Correa, J. A. (2016). Microbiota influences morphology and reproduction of the brown alga *Ectocarpus* sp. *Front. Microbiol.* 7:197. doi: 10.3389/fmicb.2016.00197

Tourneroche, A., Lami, R., Hubas, C., Blanchet, E., Vallet, M., Escoubeyrou, K., et al. (2019). Bacterial–fungal interactions in the kelp endomicrobiota drive autoinducer-2 quorum sensing. *Front. Microbiol.* 10:1693. doi: 10.3389/fmicb.2019.01693

Vallet, M., Strittmatter, M., Murúa, P., Lacoste, S., Dupont, J., Hubas, C., et al. (2018). Chemically-mediated interactions between macroalgae, their fungal endophytes, and protistan pathogens. *Front. Microbiol.* 9:3161. doi: 10.3389/fmicb.2018.03161

Wahl, M., Goecke, F., Labes, A., Dobretsov, S., and Weinberger, F. (2012). The second skin: ecological role of epibiotic biofilms on marine organisms. *Front. Microbiol.* 3:292. doi: 10.3389/fmicb.2012.00292

Wichard, T., Charrier, B., Mineur, F., Bothwell, J. H., Clerck, O. D., and Coates, J. C. (2015). The green seaweed Ulva: a model system to study morphogenesis. *Front. Plant Sci.* 6:72. doi: 10.3389/fpls.2015.00072

Williams, P. (2007). Quorum sensing, communication and cross-kingdom signalling in the bacterial world. *Microbiology* 153, 3923–3938. doi: 10.1099/mic.0.2007/012856-0

Winson, M. K., Camara, M., Latifi, A., Foglino, M., Chhabra, S. R., Daykin, M., et al. (1995). Multiple N-acyl-L-homoserine lactone signal molecules regulate production of virulence determinants and secondary metabolites in *Pseudomonas aeruginosa*. *Proc. Natl. Acad. Sci. U.S.A.* 92, 9427–9431. doi: 10.1073/pnas.92.20.9427

Yang, Z., Rogers, L. M., Song, Y., Guo, W., and Kolattukudy, P. E. (2005). Homoserine and asparagine are host signals that trigger in planta expression of a pathogenesis gene in Nectria haematococca. *Proc. Natl. Acad. Sci. U.S.A.* 102, 4197–4202. doi: 10.1073/pnas.0500312102

Young, C. A., Felitti, S., Shields, K., Spangenberg, G., Johnson, R. D., Bryan, G. T., et al. (2006). A complex gene cluster for indole-diterpene biosynthesis in the grass endophyte *Neotyphodium lolii*. *Fungal Genet. Biol.* 43, 679–693. doi: 10.1016/j.fgb.2006.04.004

Zask, A. (1992). Preparation and reaction of dilithio-2,4-oxazolidinedione with .alpha.-halo ketones. A versatile synthesis of 3-hydroxy-2(5H)-furanones. *J. Organ. Chem.* 57, 4558–4560. doi: 10.1021/jo00042a045

Zhang, Y. F., Zhang, H., He, L., Liu, C., Xu, Y., and Qian, P. Y. (2012). Butenolide inhibits marine fouling by altering the primary metabolism of three target organisms. *ACS Chem. Biol.* 7, 1049–1058. doi: 10.1021/cb200545s

Zhao, J., Chen, M., Quan, C. S., and Fan, S. D. (2015). Mechanisms of quorum sensing and strategies for quorum sensing disruption in aquaculture pathogens. *J. Fish Dis.* 38, 771–786. doi: 10.1111/jfd.12299

Conflict of Interest: The authors declare that the research was conducted in the absence of any commercial or financial relationships that could be construed as a potential conflict of interest.